Appl. Phys. B 86, 327–331 (2007)
DOI: 10.1007/s00340-006-2457-x

Applied Physics B
Lasers and Optics

Z.-H. ZHU✉
W.-M. YE
J.-R. JI
X.-D. YUAN
C. ZEN

Enhanced transmission and directional emission via coupled-resonator optical waveguides

Research Center of Photonic Crystals, National University of Defense Technology, Changsha 410073, Hunan, P.R. China

Received: 31 May 2006/Revised version: 29 August 2006
Published online: 6 October 2006 •

ABSTRACT We propose a novel photonic crystal waveguide configuration consisting of coupled-resonator optical waveguides at the termination to obtain enhanced transmission and beaming of light. We show theoretically that such a configuration can collimate the light output from a photonic crystal waveguide over a wide bandwidth range. The mechanism explained in this paper may be easily extrapolated to the photonic crystal configuration of air holes in a dielectric substrate.

PACS 42.70.Qs; 42.79.Ci

1 Introduction

The diffraction limit is a basic principle in optics. According to standard diffraction theory, the light of wavelength λ exiting from a region much smaller than $\lambda/2$ undergoes a strong angular spread and fills out the whole 2π solid angle [1]. Very recently, however, it was shown that enhanced transmission and beaming of light could be achieved by two different kinds of photonic crystal structures [2–7], one of which consists of a periodic array of corrugations at the photonic crystal (pc) termination [8–11], and the other is designed with two defects at the termination [12]. For the first kind of photonic crystal structure, the source of the enhanced transmission and beaming of light lies in that the photonic crystal corrugation interface may support a surface mode provided that an appropriate corrugation period has been selected. For the second kind of photonic crystal structure, the mechanism of directional emission is that the resulting optical field distribution at the waveguide exit resembles a triple point source, the light can emit with a low angular divergence.

Coupled-resonator optical waveguides (CROWs) [13–16] are a special optical component for integrated photonic circuits. They are constructed, in general, with a chain of strongly confined point defects or cavities. Since it was proposed in 1999, CROWs constructed in photonic crystals have attracted much attention. In CROWs, electromagnetic wave propagation is achieved via photon hopping between strongly confined neighboring cavities. Compared with the ordinary waveguides constructed by introducing line defects photonic crystals, CROWs have many peculiar optical characteristics and application, for example, highly efficient transmission [17], low group velocity, large optical field amplitude [18], pulse compression [19, 20], highly wavelength dependent delay line [21], and enhancement of stimulated emission [22].

In this paper, we propose a novel application of CROWs to obtain enhanced transmission and beaming of light by placing CROWs at the termination of the photonic crystal configuration. The main advantage of our configuration is that the frequencies of the beaming of light ranges over a wide bandwidth.

2 Structure and principle of operation

As a photonic band-gap (PBG) system, we consider a square lattice of dielectric rods in air. The relative dielectric constant of the dielectric rods is 11.56 (corresponding to the relative dielectric constant of InGaAsP-InP semiconductor material system at a 1.55 μm wavelength) and the cross-section radius is chosen to be equal to $0.18a$, where a is the lattice constant. For TE polarization with the electric field parallel to the rod axis, the photonic bandgap of the pc structure is in the normalized frequency ($\omega a/2\pi c$) range between 0.302 and 0.443 as calculated by the plane wave expansion (PWE) method, where ω and c are the angular frequency and the velocity of light in a vacuum, respectively. All results presented are for TE polarization and have been obtained with the 2D FDTD with perfectly matched layer boundary conditions. The simulations use 20×20 grid points per unit cell.

A waveguide is constructed in the structure by removing one row of the rods along the z-direction, as shown in Fig. 1a and b. CROWs are created by removing some rods at regular intervals of $2a$ at the pc termination. Details of the structure is shown in Fig. 1b. We launched continuous-wave (cw) signals with a normalized frequency of 0.392 into the photonic crystal waveguide. The output field distributions of the photonic crystal structure with and without CROWs respectively, at the pc termination, can be obtained as shown in Fig. 2a,b. On comparing Fig. 2a with b, we can find that the angular divergence of the output beam is significantly narrowed by introducing CROWs at the pc termination. The physics underlying the beaming of light can be explained qualitatively.

✉ Fax: +86-0731-4221547, E-mail: zzhwcx@163.com

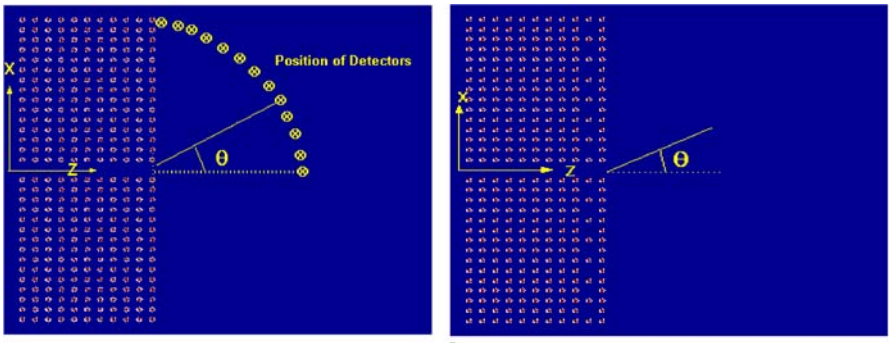

FIGURE 1 The structure and relative dielectric constant distributions by our FDTD calculation. A square lattice of dielectric rods in air. The relative dielectric constant of dielectric rods is 11.56 and the cross-section radius is chosen as $0.18a$, where a is the lattice constant. (**a**) Without CROWs at the pc termination. (**b**) With CROWs at the pc termination

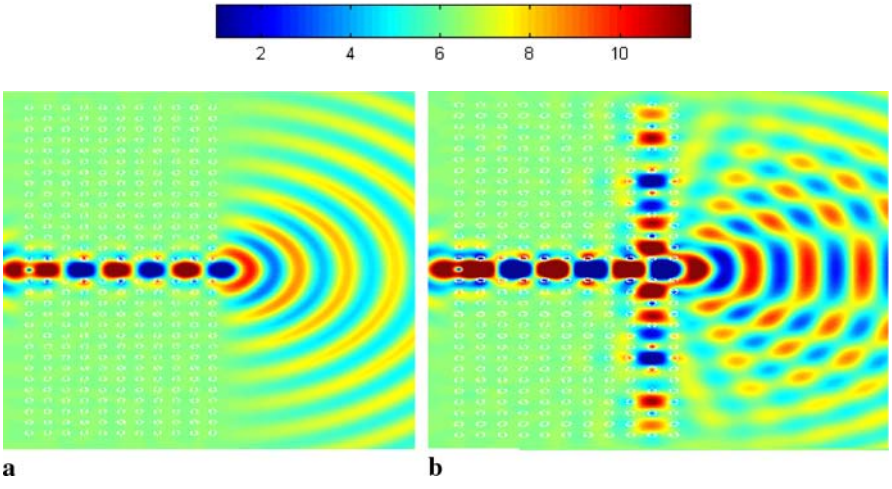

FIGURE 2 Electric-field distributions of two different photonic crystal structures. (**a**) Without CROWs at the pc termination. (**b**) With CROWs at the pc termination

These CROWs produce resonant modes, which radiate off the pc structure. These resonant modes and the optical field emitted by the pc waveguide can be regarded as radiating sources. Light radiation from these radiating sources interferes in free space. The interference produces a directional emitting beam and also several weak lateral lobes of radiation as shown in Fig. 2b.

3 Performance analysis

To study the bandwidth of the beaming of light, we launch two similar pulses into the pc waveguide with and without CROWs at the pc termination, respectively. The temporal change of the field intensity from the detectors is then recorded. The distance between the detectors and the output port of the waveguides is $15a$, as shown in Fig. 1a. By FFT transforming, we obtain the frequency spectrum of the electric field for each corresponding detector. Figure 3 shows the spectrum obtained by the detectors at the angles of 0° to 90°with an angle interval of 10°(Fig. 3a corresponding to the Fig. 1a case, and Fig. 3b corresponding to the Fig. 1b case). The intensity of the optical field for different output angles can be analyzed. For the Fig. 1b case, we can observe that the intensity difference between the detectors changes significantly as the frequency of the light in the normalized frequency range between 0.376 and 0.403, which can not be seen in the Fig. 1a case. So, beaming of light can be obtained over a wide bandwidth range by introducing CROWs at the pc termination. The mechanism providing a large operational bandwidth is due to the lower Q factor of the CROWs, which are placed near the terminating surface, and radiative losses are large. The ripples at the normalized frequency from 0.315 to 0.415 in Fig. 3 may be due to the finite length of the waveguide that causes the Fabry–Perot effect.

To study the diffraction efficiency of the directional emitting beam, we launch continuous-wave (cw) signals with a normalized frequency of 0.391 into the photonic crystal waveguide. The electric-field amplitude $|E(z, x)|$ distributions with and without CROWs at the pc termination can be obtained, respectively, as shown in Fig. 4b and c. Comparing Fig. 4b with c, we can find that the beaming of light and the higher coupling efficiency between the waveguide and air can be obtained by introducing CROWs at the pc termination. This is more clearly seen in Fig. 4a, showing the far-field radial component of the Poynting vector rS_r as a function of azimuthal angle θ.

Another interesting effect found in the system is that the structure is capable of presenting enhanced transmission when the CROWs are introduced at the input surface, by removing some rods at regular intervals of $2a$. A TE-polarized light with a normalized frequency of 0.4067 is launched into the photonic crystal waveguide. The width of the launched beam is $23a$. In Fig. 5b and c we show the electric-field amplitude $|E(z, x)|$ normalized to unity distributions of the photonic crystal structure without and with CROWs at the input surface, respectively. Comparing Fig. 5b with c, we find that enhanced transmission can be obtained by introducing CROWs at the input surface. This is more clearly seen in Fig. 5a, showing the transmission normalized to unity through a waveguide as a function of normalized frequencies. The

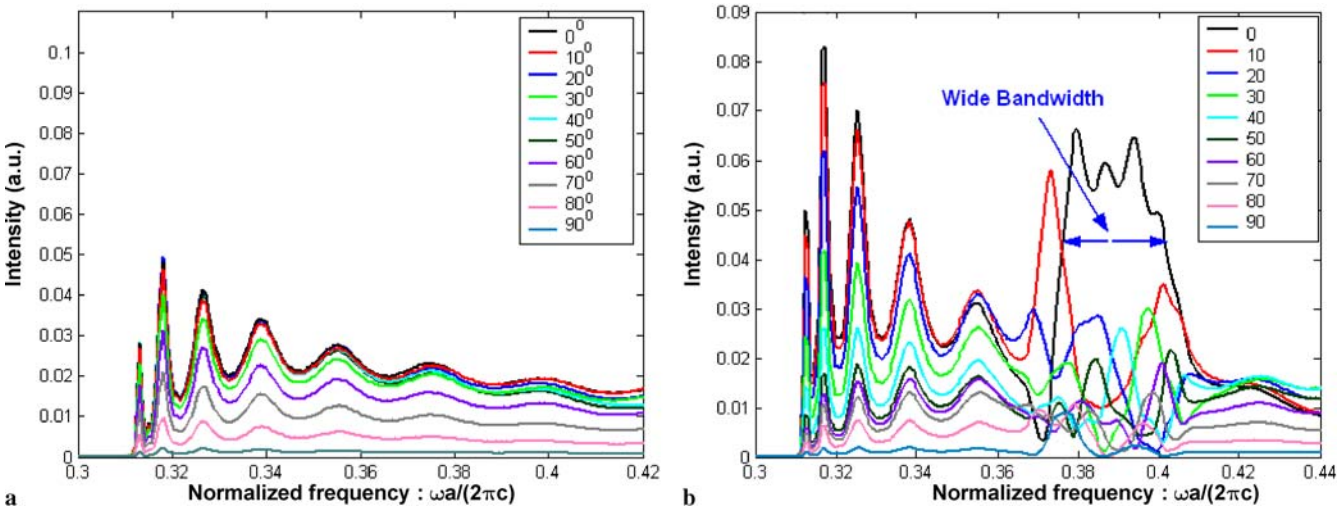

FIGURE 3 Spectra obtained by the detectors at the angles of 0° to 90° with an angle interval of 10°. (**a**) Without CROWs at the pc termination. (**b**) With CROWs at the pc termination

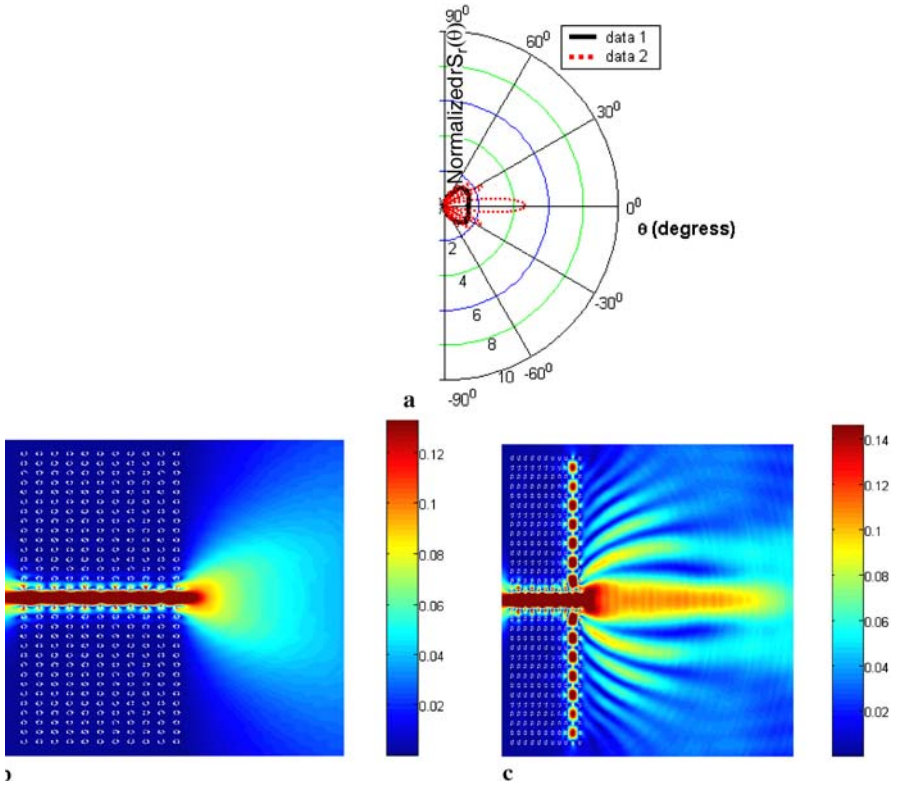

FIGURE 4 (**a**) Far-field radial component of the Poynting vector S_r as a function of azimuthal angle θ. In all cases, $rS_r(\theta)$, is normalized to unity; the "data 1" curve corresponds to the photonic crystal structure without CROWs at the pc termination, and the "data 2" curve corresponds to the photonic crystal structure with CROWs at the pc termination. (**b**) The electric-field amplitude $|E(z, x)|$ distribution of the photonic crystal structure without CROWs at the pc termination. (**c**) The electric-field amplitude $|E(z, x)|$ distribution of the photonic crystal structure with CROWs at the pc termination

"data 2" curve corresponds to the photonic crystal structure without the CROWs at the input surface, whereas the "data 1" curve corresponds to the photonic crystal structure with the CROWs at the input surface. In both curves shown in Fig. 5a, low transmission outside the PBG is due to the EM field permeating through the crystal, while the region of high transmission inside the gap is due to propagation through the waveguide. In particular, Fig. 5 shows a large resonant transmission inside the gap for the pc with CROWs at the input surface. The physics underlying the enhanced transmission can also be explained qualitatively. These CROWs produce resonant modes, and the incident waves can easily be coupled into CROWs. Since the resonant modes and the waveguide mode can easily couple to each other, enhanced transmission can be obtained.

The mechanism explained for the photonic crystal structure of dielectric rods in air may be easily extrapolated to the photonic crystal configuration of air holes in a dielectric substrate. The air-holes are hexagonally arranged in a substrate with a relative dielectric constant of 13 (corresponding to the relative dielectric constant of GaAs semiconductor material at a 1.55 μm wavelength). The radius of the air-holes is $0.48a$. The dielectric substrate is terminated by air. CROWs are added by removing some rods at regular intervals of $\sqrt{3}a$ (a is the lattice constant) at the pc termination, as shown in Fig. 6a. A TE-polarized light with a normalized frequency of

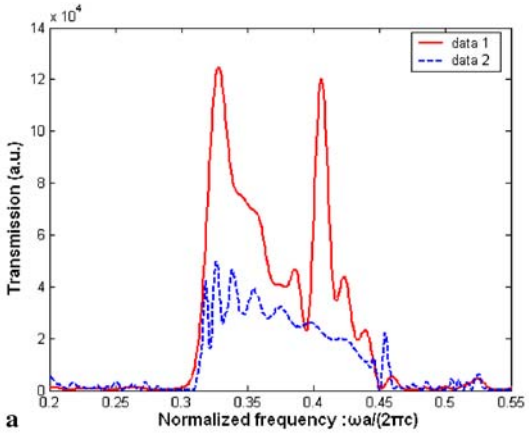

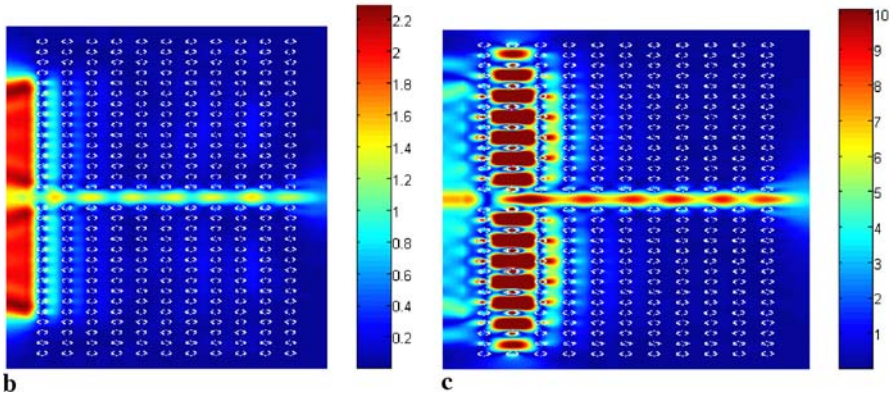

FIGURE 5 (**a**) The transmission through a waveguide as a function of normalized frequencies. The "data 2" curve corresponds to the photonic crystal structure without CROWs at the input surface, and the "data 1" curve corresponds to the photonic crystal structure with CROWs at the input surface. (**b**) The electric-field amplitude $|E(z, x)|$ distribution of the photonic crystal structure without the CROWs at the input surface. (**c**) The electric-field amplitude $|E(z, x)|$ distribution of the photonic crystal structure with the CROWs at the input surface

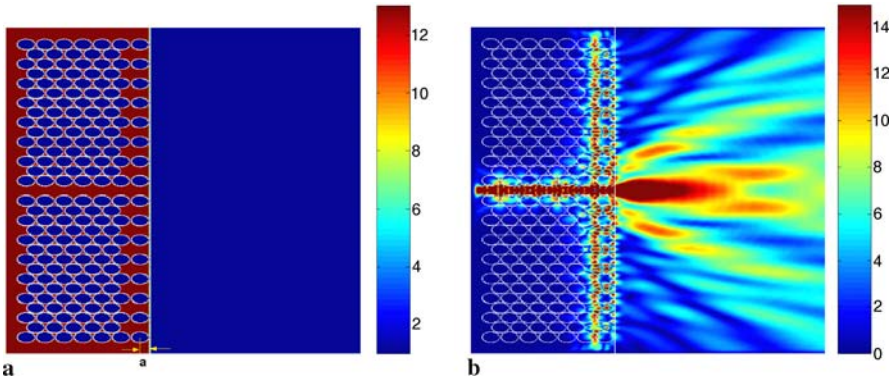

FIGURE 6 (**a**) The structure and relative dielectric constant distribution by our FDTD calculation. The air-holes are hexagonally arranged in a substrate with a relative dielectric constant of 13. The radius of the air-holes is $0.48a$. The output of the waveguide is terminated by an interface between the substrate and air. (**b**) The electric-field amplitude $|E(z, x)|$ distribution of the photonic crystal structure

$0.496(\omega a/2\pi c)$ is launched into the pc waveguides. In Fig. 6b the electric-field amplitude $|E(z, x)|$ distribution of the structure is shown. We can observe resonant modes at the defects and the fact that the output beam is directionally emitted.

4 Conclusion

In this paper, we have proposed novel pc structures for obtaining enhanced transmission and beaming of light. We demonstrated that very narrow beams can be achieved by introducing CROWs at the pc termination, and enhanced transmission can also be obtained when the CROWs are introduced at the input surface. The mechanism explained in this paper may be easily extrapolated to the photonic crystal configuration of air holes in a dielectric substrate. The enhanced transmission and beaming of light property could have some interesting applications in enhancing the light coupling efficiency from pc waveguides to conventional waveguides or conventional optical fibers, while narrowing the beam divergence of the edge emitting pc lasers.

REFERENCES

1 H.A. Bethe, Phys. Rev. **66**, 163 (1944)
2 E. Yablonovitch, Phys. Rev. Lett. **58**, 2059 (1987)
3 S. John, Phys. Rev. Lett. **58**, 2486 (1987)
4 O. Painter, R.K. Lee, A. Scherer, A. Yariv, J.D. O'Brien, P.D. Dapkus, I. Kim, Science **284**, 1819 (1999)
5 J.D. Joannopoulos, P.R. Villeneuve, S. Fan, Nature **386**, 143 (1997)
6 M. Soljacic, J.D. Joannopoulos, Nature Mater. **3**, 211 (2004)
7 K.M. Leung, Y.F. Liu, Phys. Rev. Lett. **65**, 2646 (1990)
8 E. Moreno, F.J. García, L. Martin-Moreno, Phys. Rev. B **69**, 121 402 (2004)
9 H.J. Lezec, A. Degiron, E. Devaux, R.A. Linke, L. Martin-Moreno, F.J. Garcia-Vidal, T.W. Ebbesenl, Science **297**, 820 (2002)
10 P. Kramper, M. Agio, C.M. Soukoulis, A. Birner, F. Müller, R.B. Wehrspohn, U. Gösele, V. Sandoghdar, Phys. Rev. Lett. **92**, 113 903 (2004)

11 S.K. Morrison, Y.S. Kivshar, Appl. Phys. Lett. **86**, 081 110 (2005)
12 C.-C. Chen, T. Pertsch, R. Iliew, F. Lederer, A. Tünnermann, Opt. Express **14**, 2423 (2006)
13 A. Yariv, Y. Xu, R.K. Lee, A. Scherer, Opt. Lett. **24**, 711 (1999)
14 M. Bayindir, B. Temelkuran, E. Ozbay, Phys. Rev. Lett. **84**, 2140 (2000)
15 S. Olivier, C. Smith, M. Rattier, H. Benisty, C. Weisbuch, T. Krauss, R. Houdre, U. Oesterle, Opt. Lett. **26**, 1019 (2001)
16 T.D. Happ, M Kamp, A. Forchel, J. Gentner, L. Goldstein, Appl. Phys. Lett. **82**, 4 (2003)
17 M. Bayindir, B. Temelkuran, E. Ozbay, Phys. Rev. B **61**, R11 855 (2000)
18 H. Altug, J. Vuèkoviæ, Appl. Phys. Lett. **84**, 161 (2004)
19 A. Martinez, A. Garcia, P. Sanchis, J. Marti, J. Opt. Soc. Am. A **20**, 147 (2003)
20 T.J. Karle, Y.J. Chai, C.N. Morgan, I.H. White, T.F. Krauss, J. Lightwave Technol. **22**, 514 (2004)
21 M. Bayindir, E. Ozbay, Opt. Express **10**, 1279 (2002)
22 K. Sakoda, Opt. Express **4**, 167 (1999)